Theoretical analysis of the low-voltage cascade electro-osmotic pump

Anders Brask, Goran Goranović, Henrik Bruus[*]

Mikroelektronik Centret (MIC), Technical University of Denmark, DK-2800 Kongens Lyngby, Denmark

Abstract

The recently published experimental results obtained by Takamura et al. [Y. Takamura, H. Onoda, H. Inokuchi, S. Adachi, A. Oki, Y. Horiike, in: J.M. Ramsey, A. van den Berg (Eds.), Proceedings of the μTAS 2001, Monterey, CA, USA, Kluwer Academic Publishers, Drodrecht, 2001, p. 230], on their low-voltage cascade electro-osmotic pump are analyzed using two different theoretical approaches. One is the semi-analytical equivalent circuit theory involving hydraulic resistances, pressures, and flow rates. The other is a full numerical simulation using computational fluid dynamics. These two approaches give the same results, and they are in good qualitative agreement with the published data. However, our theoretical results deviate quantitatively from the experiments. The reason for this discrepancy is discussed.
© 2003 Elsevier Science B.V. All rights reserved.

1. Introduction

Micropumps play a key role in the quest for fabricating versatile, cheap, and highly efficient microfluidic lab-on-a-chip devices. In this growing field especially micropumps based on electroosmotic flow (EOF) [1–3] are becoming important [4–9]. They contain no moving parts and are compact. Moreover, they are relatively easy to integrate in microfluidic circuits during fabrication.

One major drawback in the conventional design of EOF micropumps is the use of high voltage to drive the pump. The invention in 2001of the low-voltage cascade EOF pump by Takamura et al. [5] therefore marks an interesting development in the field. In the future, EOF pumps may be powered by battery; and hence, portable.

The aim of our work is two-fold. (1) We want to provide the first theoretical analysis of the experimental results obtained by Takamura et al. [5,10]. (2) Using computational fluid dynamics (CFD) we want to demonstrate that the complex EOF pump is adequately described by the semi-analytical equivalent circuit theory involving hydrodynamic resistances, pressures, and flow rates. Both calculational methods are approximate, but since they are independent

and yield comparable results, we have gained confidence in our theoretical results.

2. Principles of the EOF pump

To set the stage for our analysis we briefly recapitulate the working principles of the low-voltage cascade EOF pump [5]. The pump is designed to work as an effective pressure source for low applied voltages. The layout of the pump is shown in Fig. 1.

The main principle is to connect multiple EOF pumps in series in order to accumulate pressure. Each elementary EOF pump (denoted a step) consists essentially of a narrow channel section, marked B in Fig. 1, containing 10 parallel channels, followed by a wide channel section, marked C in Fig. 1, containing a single channel. The EOF in the narrow channel section acts as a high pressure pump with forward electric field. In the wide channel section the electric field is reversed, but here the channel is so wide that the induced back pressure is small compared to the previous pressure. After flowing through one such pump step the accumulated voltage is thus zero, while an appreciable pressure is maintaining a net flow. This ensures EOF pumping using a low operating voltage, indeed an attractive feature allowing the pump to be operated with a battery and thus to be portable. Furthermore, it is more safe to use low voltages.

---
[*] Corresponding author. Tel.: +45-4525-6399; fax: +45-4588-7762.
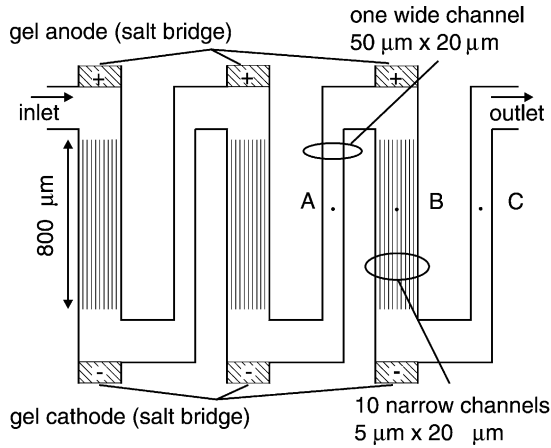*E-mail address:* bruus@mic.dtu.dk (H. Bruus).

Fig. 1. Top view of the low-voltage cascade EOF pump with three steps (adapted from Fig. 3 in [5]). The total pressure is proportional to the number of steps. The EOF is driven through many parallel narrow channels by a forward electric field and through one wide channel with a reversed electric field. A net flow is thus generated without accumulation of voltage.

The disadvantage of a cascade pump is the extra complexity of the many electrodes.

We begin our analysis by noting that water at room temperature has the kinematic viscosity $v = 10^{-6}$ m²/s, and when, as in the experiment, it flows with the velocity $u \approx 10^{-3}$ m/s through a channel of width $D = 50$ μm, the Reynolds number, Re, is minute:

$$Re = \frac{uD}{v} = 0.05. \tag{1}$$

For such a low Reynolds number the flow is laminar and the viscous forces are dominant. In the case of uniform flow, i.e. zero spatial derivatives in the flow direction, the Navier-Stokes equation becomes linear.

In this limit, for a steady-state flow through a channel with a hydraulic resistance R_{hyd}, the flow rate Q_{hyd} induced by the pressure drop Δp_{hyd} is

$$Q_{hyd} = \frac{\Delta p_{hyd}}{R_{hyd}}. \tag{2}$$

Polar liquids offer another possibility beyond pure hydro-dynamics to generate a flow: namely the electrically driven EOF [1–3]. Ions in the liquid form a thin (<100 nm) electric double layer, the Debye layer, at the walls of the channel, and when an electric potential drop $\Delta\phi_{eo}$ is applied along the channel an EOF is initiated. In the limit of infinitely thin Debye layers, the flow velocity u_{eo} at the walls is given by the Smoluchowski expression

$$u_{eo} = \mu_{eo} \frac{\Delta\phi_{eo}}{L}, \tag{3}$$

where μ_{eo} is the so-called electroosmotic mobility, and L the length of the channel. For a pure EOF, the flow rate Q_{eo} in a channel with cross-sectional area A is given by

$$Q_{eo} = u_{eo}A = \mu_{eo} \frac{\Delta\phi_{eo}}{L} A \frac{R_{hyd}}{R_{hyd}} \equiv \frac{\Delta p_{eo}}{R_{hyd}}, \tag{4}$$

where R_{hyd} and the EOF pressure Δp_{eo} is introduced in the second and third equality, respectively, so that Q_{eo} appears as Q_{hyd} in Eq. (2). In accordance with [6], Δp_{eo} is thus defined by:

$$\Delta p_{eo} = \mu_{eo} \Delta\phi_{eo} R_{hyd} \frac{A}{L} = \mu_{eo} \Delta\phi_{eo} R_{hyd} \frac{\rho_{el}}{R}, \tag{5}$$

where the geometry ratio A/L equals the ratio between the electric resistivity ρ_{el} of the liquid phase and the electric resistance R of the channel.

Equivalently, Δp_{eo} can be defined as the hydraulic back pressure needed to balance an EOF, i.e.$|Q_{eo}| = |Q_{hyd}|$. The total flow rate Q of a channel with both a pressure-driven flow and an EOF is simply

$$Q = Q_{eo} + Q_{hyd} = \frac{\Delta p_{eo} + \Delta p_{hyd}}{R_{hyd}}. \tag{6}$$

Likewise, the resulting velocity profile is given by a super-position of the velocity profiles of the EOF and the pressure-driven flow, respectively [2].

Consider a pump in a fluidic network. If the back pressure Δp_{hyd} is zero, the flow is denoted a "free run flow" and the corresponding flow rate is termed Q_{max}. The counter pressure needed to stop the flow (i.e.$Q = 0$) through the entire pump is denoted the maximum back pressure p_{max}.

3. Analysis of the EOF pump

From Eq. (5), it follows that the EOF-induced pressure buildup is very large in the narrow channel section, and thus the flow profile in this section becomes only slightly deformed under the influence of the actual back pressure. The resulting velocity profile u_1, shown in Fig. 2, is a sum of a large, positive
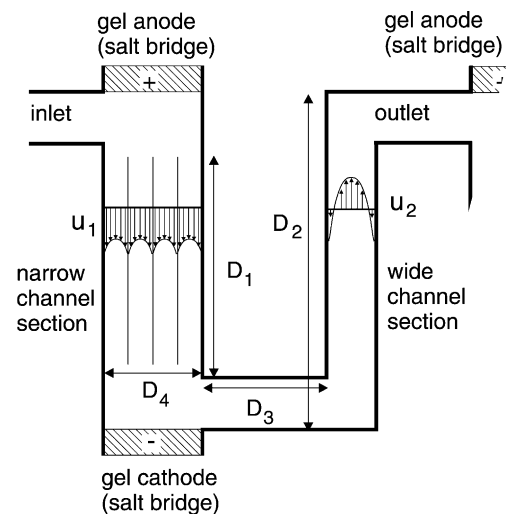

Fig. 2. Simplified schematics of one step of the cascade EOF pump shown in Fig. 1. The flow profiles in both narrow and wide channels are shown. There are 10 channels in the narrow channel section, but for clarity only 4 are depicted. Even though the flow is reversed near the wall in the wide channel, the net flow is still positive. The parameters taken from [5] are: $D_1 = 800$ μm, $D_2 = 1230$ μm, $D_3 = 170$ μm, and $D_4 = 185$ μm.

and flat EOF velocity profile and a small, negative and parabolic back pressure velocity profile. The pressure buildup in the narrow channel section is denoted Δp_{eo}^N.

In the wide channel the electric field is reversed. A part of the pressure generated in the narrow section is therefore used both for overcoming the reversed, small, and flat EOF profile and for driving the flow by pressure. The resulting velocity profile is the large, forward parabolic-like velocity profile u_2 shown in Fig. 2. It is evidently imperative to make the channel width considerably larger in this section to keep its back pressure to a minimum. The pressure drop in the wide channel section is denoted Δp_{eo}^W.

The final pressure buildup Δp_{step}^{max} along the whole step is the EOF pressure buildup in the narrow channel section minus the back pressure drop in the wide channel section,

$$\Delta p_{step}^{max} = \Delta p_{eo}^N - \Delta p_{eo}^W. \tag{7}$$

3.1. Equivalent circuit theory

The concepts from the previous section can be used to analyze the pump using the so-called equivalent circuit theory. In this theory, the hydraulic resistance of a fluidic network is calculated by representing individual sections with equivalent hydraulic resistors using the usual rules for series and parallel resistors. The flow rate and the pressure drop for a hydraulic resistor are related by Eq. (2). For details see [6].

The equivalent circuit theory is only exact for a uniform and laminar flow. Hence, it is not possible to analyze the flow near a bend. In the following analysis the bends are neglected, an approximation justified in Section 3.2 by CFD simulation.

The first step is to find the equivalent diagram for the pump. It consists of a parallel coupling of $N = 10$ identical resistors $R_{hyd,1}$ followed by $R_{hyd,3}$ and $R_{hyd,2}$ in series as shown in Fig. 3b. For a single rectangular channel of width W and height H, R_{hyd} is given by [6],

$$R_{hyd} = \frac{12\eta L H^{-4}}{(W/H) - \sum_{m=0}^{\infty}(192/(\pi^5(2m+1)^5))\tanh\left[((2m+1)\pi W)/2H\right]}, \tag{8}$$

where η is the dynamic viscosity. $R_{hyd,1}$ and $R_{hyd,2}$ are then computed using Eq. (8). The short channel connecting the narrow and wide channel sections can safely be neglected,

since $R_{hyd,3} \ll R_{hyd,1}, R_{hyd,2}$. The total hydraulic resistance R_{hyd}^{total} is therefore given as

$$R_{hyd}^{total} = N^{-1}R_{hyd,1} + R_{hyd,2}. \tag{9}$$

To drive the EOF an external electrical potential, $\Delta\phi_{ch}$, is applied to the resistor network (Fig. 3a). Only a fraction α of $\Delta\phi_{ch}$ is dropped over the EOF channels. This effective potential drop is denoted $\Delta\phi_{eo}$,

$$\Delta\phi_{eo} = \alpha\,\Delta\phi_{ch}. \tag{10}$$

Using the circuit diagram we determine α. The electrical resistance of a single rectangular channel with length L, width W, and height H is given by

$$R = \rho_{el}\frac{L}{HW}. \tag{11}$$

Combining this with the actual geometry of Fig. 1, it follows that

$$\alpha = \frac{(N/R_1 + 1/R_2)^{-1}}{(N/R_1 + 1/R_2)^{-1} + R_3} = 0.885. \tag{12}$$

The actual applied potential $\Delta\phi_{app}$ does not equal $\Delta\phi_{ch}$ because further potential drops occur in the gel electrodes. Hence, $\Delta\phi_{eo}$ is unknown but could have been estimated if the electrical current and conductivity of the liquid had been measured experimentally.

At this point the EOF pressures Δp_{eo}^W, Δp_{eo}^N, and Δp_{step} can be found for a given potential. However, it remains to verify the validity of the approximate equivalent circuit theory. This is done by numerical simulations in the following.

3.2. Computational fluid dynamics

A full numerical simulation was performed using the commercial computational fluid dynamics program Coven-

tor 2001.3. The program can simulate EOF in the limit of infinitely thin Debye layers. The electric potential is calculated first, and by the Smoluchowski relation Eq. (3) it is used to establish the boundary conditions for the velocity field at the walls. The accuracy of the CFD could be measured for straight channels with rectangular cross-section, since there the equivalent circuit model gives analytical answers.

In order to save calculation time, it is important to identify the minimal computational domain. Only one pump step needs to be analyzed. Further simplifications can be achieved by symmetry considerations. Clearly, the pump is symmetric about the horizontal plane at half the channel depth. Due to the very low Reynolds number, $Re < 0.05$, the flow is said to be creeping. Numerical investigation by Yang
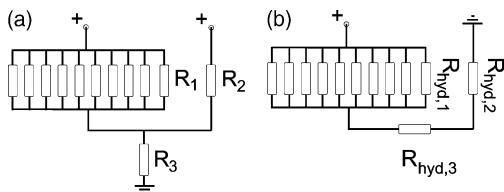

Fig. 3. (a) The equivalent electrical circuit used in the calculation of potential drop across the EO section. (b) The slightly different equivalent circuit for the fluidic network used in the calculation of flow rates. There are $N = 10$ narrow channels each with the hydraulic resistance $R_{hyd,1}$. In our calculations $R_{hyd,3}$ is neglected.

et al. [11] showed that for a 90° bend, inertial effect was negligible for $Re < 5$. Consequently, it does not matter which way the liquid flows. The flow pattern in the first half of a pump step (e.g. between A and B in Fig. 1) therefore equals that in the second half (e.g. between B and C in Fig. 1). Hence, only half of the computational domain needs to be considered. This was verified by a full-geometry simulation. The flow rate and pressure buildup for the complete pump step are twice the values obtained using the symmetry-reduced geometry.

The CFD simulation was done with various grids to find those yielding grid-independent results. We focused especially on problems at the corners, since they are known to be problematic [12]. We ended using a grid containing 10^5 rectangular cells with 14×7 cells in each cross-section. The CFD results for this grid matched the analytical circuit model within 5%.

4. Results and discussion

4.1. Velocity profiles

A simulation of the low-voltage cascade EOF pump gave the velocity profiles depicted in Fig. 4. There is one profile for the wide channel, and one for a single narrow channel. The profiles have been extracted from the symmetry plane. The CFD program solves the Poisson equation for a given potential drop $\Delta\phi_{ch}$ and finds that the electric fields are slightly different in the wide and narrow channels. In the circuit model they are assumed to be the same. The calculated velocity profiles at two positions are sketched in Fig. 2.
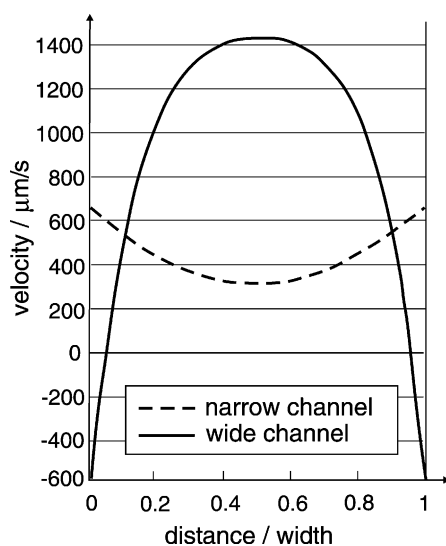

Fig. 4. CFD simulated velocity profiles at the symmetry plane in a wide and a narrow channel. The velocity at the walls is the EOF velocity. The parameters are: $\eta = 1.00 \times 10^{-3}$ Pa s, $\mu_{eo} = 0.06$ mm^2/(V s), and $\Delta\phi_{ch} = 10$ V.

4.2. Comparison with experiments

The circuit model is now used to calculate the back pressure p_{max} and the EOF velocity u_{eo} as a function of the potential drop. Unfortunately, neither the actual potential drop $\Delta\phi_{ch}$ nor the EOF mobility μ_{eo} was measured in the experiment. However, both back pressure and flow velocity depend linearly on the product $\mu_{eo}\,\Delta\phi_{ch}$, and, as we shall see, this makes a comparison between experiments and theory possible.

In the case of a 15-step cascade pump, Takamura et al. [5] measured a max back pressure of 800 Pa and for the same voltage and under free run conditions, a max velocity $u_{max} = 0.50$ mm/s. The velocity measurements were conducted in the last wide section, which had no electric field. Hence, the flow is solely pressure driven.

The relation between the back pressure and the product $\mu_{eo}\,\Delta\phi_{ch}$ is found using Eqs. (5) and (7), and it is plotted in Fig. 5. From the figure, it is found that the measured 800 Pa corresponds to $\mu_{eo}\,\Delta\phi_{ch} = 0.114$ mm^2/s. Using this value the model predicts the flow rate $Q_{max} = 0.110$ nl/s. From this flow rate, the maximum velocity u_{max} may be calculated in the wide channel section.

Using the aspect ratio as a variable parameter, we performed a general analysis of the relation between flow rates and maximal flow velocities in rectangular channels with cross-section area A. For the actual aspect ratio $W/H = 2.5$ we found a numerical factor 0.52:

$$u_{max} = \frac{Q_{max}}{0.52\,A} = 0.21\,\text{mm/s}, \tag{13}$$

where $A = 50 \times 20\ \mu m^2$. This velocity, found both by simulation and by the circuit model, deviates by a factor 2.4 from the measured 0.50 mm/s.

In [5], results from a 6-step and 15-step pump are presented. The back pressure measurements give 380 and 860 Pa for the 6-step and 15-step pump, respectively, at $\phi_{app} = 25$ V. The corresponding ratio is then $860/380 = 2.26$ which should be compared with $15/6 = 2.5$. Hence, it can be concluded that the pressure is not accumulated linearly with the number of steps in contrast to theoretical expectations. The deviation may be within the range of uncertainty for the pressure measurements.

To obtain realistic estimates for the absolute values of the EOF pump parameters, we use some typical values for μ_{eo} and $\Delta\phi_{ch}$. The results for Q_{max}, p_{max}, and R_{hyd} obtained by model calculations and simulations are compared in Table 1

Table 1
Comparisons between equivalent circuit model and numerical simulation for a single pump step

	Q_{max} (nl/s)	p_{max} (Pa)	R_{hyd} (kg/(m^4 s))
Model	0.577	281.0	4.88×10^{14}
Simulation	0.560	274.0	4.89×10^{14}
Deviation	3%	2%	0%

Parameters: $\mu_{eo} = 0.06$ mm^2/(V s), $\eta = 1.0 \times 10^{-3}$ Pa s, $\Delta\phi_{ch} = 10$ V.
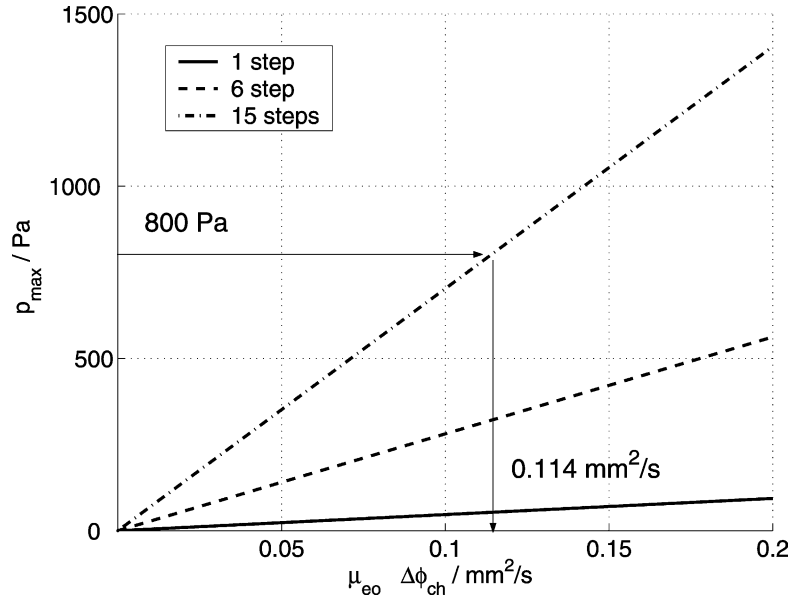
Fig. 5. Maximum back pressure as a function of $\mu_{eo} \Delta\phi_{ch}$. The pressures are calculated using the equivalent circuit theory. The one step slope is 468 Pa s / mm^2 for $\eta = 1.00 \times 10^{-3}$ Pa s, $\alpha = 0.885$. The measured pressure of 800 Pa leads to a value $\mu_{eo} \Delta\phi_{ch} = 0.114$ mm^2/s.

for a given set of parameters. The two sets of results agree well. Calculations with $\mu_{eo} = 0.06$ mm^2/(V s) give considerably larger pressures than those measured, e.g. 4200 Pa for the 15-step pump with $\Delta\phi_{ch} = 10$ V. This indicates the possibility for improving the performance of the pump.

5. Discussions and conclusions

Discussions with Takamura [10] have led to the following conclusions regarding the discrepancies between experiment and theory.

(1) The velocity mismatch of a factor of 2.4 is probably due to fabrication difficulties. The actual width of the narrow channels may have been as large as 8 μm instead of the design value of 5 μm [10]. Since $\Delta p_{eo} \propto W^{-2}$ for $W \ll H$, the pressure for a 8 μm wide channel is $(8/5)^2 = 2.6$ times smaller than for a 5 μm channel. This would lower the slopes of the lines in Fig. 5 and instead of reading off 0.114 mm^2/s on the abscissa, we would get 0.296 mm^2/s. Using this number for $\mu_{eo} \Delta\phi_{ch}$, we obtain $u_{max} = 0.55$ mm/s. This result agrees better with the observed 0.5 mm/s. A source for minor inaccuracies is the actual shape of the channel cross-section.
(2) The pressure does not increase linearly with the number of stages. Two possible explanations of this observation are: (a) due to the design of the pump the individual gel electrodes do not have the same potential; (b) pressure-dependent hydraulic resistances of the gel electrodes, i.e. leaks in the gel electrodes increases with increasing pressure.

(3) The experimental accuracy of the velocity and pressure measurements is 15–30%. Part of the discrepancies could therefore simply arise from inaccurate measurements.

The above explanations can account for the large quantitative deviations between theory and experiment, and the problems will be addressed in coming improved version of the low-voltage cascade EOF pump [10].

In summary, we have presented a simple analytical model for the low-voltage EOF pump obtained by using equivalent circuit theory. This approximate model has proved sufficient for making good estimates of the performance of the pump. Full CFD numerical simulations were made to verify the model and to provide more detailed information about the flow. The model and the simulations agree within 3%. Our theoretical analysis was compared to experimental results obtained by Takamura et al. [5], and good qualitative agreement was observed. However, a considerable quantitative deviation (a factor of 2.4) was found for values of calculated versus measured maximum velocity. The possible sources for this discrepancy were identified as inaccuracies in the measurement of various parameters (channel widths, velocities, and pressures) and pressure leakages.

Our work shows the advantage of theoretical analysis as a supplement to the experimental approach in the study of EOF pumps. Our pressure calculations indicate, for example, that there is room for improving the performance of the pump. We have also shown that, although approximate, the equivalent circuit model is applicable to the cascade EOF pump. This is mainly because the corrections from electrical and hydraulic corner effects are negligible. Use of the circuit model facilitates the analysis of the pump enormously.

Acknowledgements

References

[1] J.F. Osterle, J. Appl. Mech. 31 (1964) 161.

[2] C.L. Rice, R. Whitehead, J. Phys. Chem. 69 (1965) 4017.

[3] A. Manz, C.S. Effenhauser, N. Burggraf, D.J. Harrisson, K. Seiler, K. Fluri, J. Micromech. Microeng. 4 (1994) 257.

[4] P.H. Paul, D.W. Arnold, D.J. Rakestraw, Proceedings of the μTAS 1998, Banff, Canada, 1998, p. 49.

[5] Y. Takamura, H. Onoda, H. Inokuchi, S. Adachi, A. Oki, Y. Horiike, in: J.M. Ramsey, A. van den Berg (Eds.), Proceedings of the μTAS 2001, Monterey, CA, USA, Kluwer Academic Publishers, Drodrecht, 2001, p. 230.

[6] W.E. Morf, O.T. Guenat, N.F. de Rooij, Sens. Actuators B-Chem. 72 (2001) 266.

[7] O.T. Guenat, D. Ghiglione, W.E. Morf, N.F. d Rooij, Sens. Actuators B-Chem. 72 (2001) 273.

[8] S. Zeng, C.-H. Chen, J.C. Mikkelsen Jr., J.G. Santiago, Sens. Actuators B-Chem. 79 (2001) 107.

[9] D.R. Reyes, D. Lossifidis, P.-A. Auroux, A. Manz, Anal. Chem. 74 (2002) 2623.

[10] Experimental parameters not quoted in the original experimental paper were kindly provided by Dr. Y. Takamura, Univ. Tokyo.

[11] R.-J. Yang, L.-M. Fu, Y.-C. Lin, J. Colloid Interf. Sci. 239 (2001) 98.

[12] N.A. Patankar, H.H. Hu, Anal. Chem. 70 (1998) 1870.